

## Impacts of Titanium Dioxide Nanoparticles Used in Processing Military Protection Wears on the Skin - Ultrastructure and Molecular Study

Sameh M. Abouzead<sup>1</sup>, Nagui H. Fares<sup>2</sup>, Abdelmordy M. Mohamed<sup>2</sup> and Yomna I. Mahmoud<sup>2</sup>

<sup>1</sup>Technical Research Center of Armed Forces, Cairo, Egypt

<sup>2</sup>Zoology Department, Faculty of Science, Ain Shams University, Cairo, Egypt

[Sameh\\_abouzead@yahoo.com](mailto:Sameh_abouzead@yahoo.com)

**Abstract:** With the rapid growth of nanotechnology especially in the field of military protection wears. There are growing concerns about the toxicity of Titanium Dioxide Nanoparticles (TiO<sub>2</sub>-NPs), as they helpfully provide many valuable applications in that field. For this purpose, this work was designed to evaluate the noxious effects of TiO<sub>2</sub>-NPs on rabbits skin at the cellular and molecular levels. Three concentrations of aqueous suspensions of TiO<sub>2</sub>-NPs (0.5, 1.0 and 2.0 %) w/v were prepared and tested on the shaved skin with three exposure times (24, 48 and 72hrs) for each concentration. The histology, morphology, morphometry and ultrastructure of the skin were examined by the light and electron microscopy. In addition, to know to what extent such chemicals in the nanoform are harmful on the molecular level. Esterase patterns, general proteins and glutathione system of the skin were studied. The study demonstrates no evidence that TiO<sub>2</sub>-NPs at the doses of 0.5 % (24, 48 and 72hrs), 1.0% (24, 48hrs), and 2.0 % (24hrs) could penetrate into the deeper Stratum Corneum (SC) layers, epidermis or dermis. Thus the barrier function of the skin was successful in limiting the passage of particles. On the contrary, the present work illustrated hazardous effects after 72hrs exposure to 1.0 % concentration as well as, 48 and 72hrs exposure to 2.0 % concentration of TiO<sub>2</sub>-NPs. At the cellular level, the ultrastructure examinations revealed the penetration of these NPs through the SC layer, the penetration level increased in a time and dose dependent manner. At the molecular level, these doses showed signs of interaction with the protein contents of the skin as revealed by the disturbances in the SDS-PAGE banding pattern of general proteins, in addition, the inhibitory effect of TiO<sub>2</sub>-NPs in the ESTs and glutathione enzymes demonstrate the participation of the ROS formation and the oxidative stress in the toxicity mechanism of these NPs.

[Sameh M. Abouzead, Nagui H. Fares, Abdelmordy M. Mohamed and Yomna I. Mahmoud. **Impacts of Titanium Dioxide Nanoparticles Used in Processing Military Protection Wears on the Skin - Ultrastructure and Molecular Study.** *Life Sci J* 2015;12(5):54-70]. (ISSN:1097-8135). <http://www.lifesciencesite.com>. 7

**Keywords:** Military Protection Wears. Nanoparticles. Titanium dioxide. Toxicity. Skin. Esterase. Proteins. glutathione.

### 1- Introduction

Textiles are a very important class of materials used by the military where they rely on clothing and items made from textiles for protection and even life support. Military clothing is considered an integral part of the soldier's fighting kit (Satam, 2007).

There is a growing awareness of the importance of clothing in enhancing the performance of soldiers and protecting their lives during combat. Such awareness has prompted militaries around the world to step up their research and development efforts in an attempt to create the ideal combat uniform. This requires continuous research to provide an update on the considerable advances that have occurred in that field in recent years by using many techniques and technologies. Among these nanotechnology gives rise to an important branch of protection wears known as Nano-Treated Military Protection Wears (NTMPW) (Satam, 2007).

Nanotechnology is defined as the utilization of structures with at least one dimension of nanometer size for the construction of materials, devices or

systems with novel or significantly improved properties due to their nano-size. Nanotechnology can best be described as activities at the level of atoms and molecules that have applications in the real world. Nanoparticles (NPs) commonly used in products are in the range of 1 -100 nm (Wong, 2006).

Of all the NPs, Titanium Dioxide (TiO<sub>2</sub>) is used in processing military protection wears. This compound had anti-bacterial properties, UV radiation protection, self-cleaning, self-decontamination, fire retardant, improvement high tensile strength, wrinkle resistance...etc (Dastjerdi and Montazer, 2010, Jeevani, 2011, Senic *et al.*, 2011). Despite of these highly useful applications, such chemical may also cause hazardous effects and toxicity especially with regard to the dermal risks as the MPW are obligatory to be in direct contact with the skin.

A number of *in vitro* and *in vivo* studies have investigated the penetration of TiO<sub>2</sub>-NP through the skin. Dussert and Gooris (1997) studied water/oil (w/o) emulsions of TiO<sub>2</sub> on excised human skin and found that the emulsion remained on the surface of the

SC; however, TiO<sub>2</sub> formulations (80–200 nm, up to 1 ml) applied to *in vitro* porcine skin for 24 hr showed no penetration (Gamer *et al.*, 2006). Absorption studies with *in vitro* and *in vivo* human skin (20 nm TiO<sub>2</sub> in a w/o emulsion for 5 hrs) showed no penetration into the viable epidermal layers (Mavon *et al.*, 2007). TiO<sub>2</sub> oil/water (o/w) emulsions applied to *in vitro* human organotypic cultures for 24hrs and to *in vivo* human forearms for 6hrs (Bennat and Muller-Goymann, 2000) showed that penetration was greater *in vitro* than *in vivo*, but TiO<sub>2</sub> tape stripping indicated that particles remained within SC layers. Similar studies with hydrophobic (100 nm), amphiphilic (10–15 nm), and hydrophilic (20 nm) micronized TiO<sub>2</sub> in o/w emulsions applied nonocclusive to human forearms for 6 hrs showed formation of a thin film on the SC (Schulz *et al.*, 2002), and neither particle shape, formulation, nor exposure had a significant impact on penetration. Human foreskin grafted onto severe combined immunodeficiency (SCID) mice treated with hydrophobic emulsions of occluded micronized TiO<sub>2</sub> and analyzed by particle induced x-ray emission (PIXE) and scanning transmission ion microscopy tracked Ti particles to the stratum granulosum (SG) layer of the epidermis (Kerte'sz *et al.*, 2005).

Alternatively, Kiss *et al.* (2007) showed that no TiO<sub>2</sub>-NP penetrated intact skin of SCID models. Lekki *et al.* (2007) applied TiO<sub>2</sub> to porcine and human skin by gentle rubbing and found Ti in the upper three to five layers of the SC and to the depth of hair follicles by PIXE, concluding that mechanical movement (tensile and compressive) played a role in penetration. Studies by Lademann *et al.* (1999) reported TiO<sub>2</sub> within some follicular orifices, but most remained on the skin surface. In contrast, studies conducted 8–24hrs *in vivo* porcine skin by Menzel *et al.* (2004) suggested that hair follicles were not important but detected four different formulations of TiO<sub>2</sub> on the SC and in the SG using ion beam analysis. Tan *et al.* (1996) applied micronized TiO<sub>2</sub> in older patients for 9–31 days and detected insignificant levels of Ti in the dermis. Normal and damaged (tape stripped) skin from pigs exposed to four different types of TiO<sub>2</sub> (35–250 nm) *in vitro* for 24 hr in Franz cells showed no Ti penetration in the receptor fluid (Senzui *et al.*, 2010). Finally, three different TiO<sub>2</sub> formulations applied daily for 22 days to minipigs showed localization of TiO<sub>2</sub> in the upper SC and follicular lumen, with isolated TiO<sub>2</sub> within the dermis with all three formulations (Sadrieh *et al.*, 2010).

Consequently, the present work was designed to evaluate the noxious effects of TiO<sub>2</sub>-NPs used in the processing of the military protection wears on rabbits skin at the cellular and molecular levels. Three concentrations of aqueous suspensions of TiO<sub>2</sub>-NPs

(0.5, 1.0 and 2.0 %) w/v were prepared and tested on the shaved skin with three exposure times (24, 48 and 72hrs) for each concentration. The histology, morphology, morphometry and ultrastructure of the skin were examined by the light and electron microscopy. In addition, to know to what extent such chemicals in the nanoform are harmful on the molecular level. Esterase patterns, general proteins and glutathione system of the skin were studied.

## 2- Material and Methods

### Chemicals and Reagents

Titanium Dioxide Nanoparticles (TiO<sub>2</sub>-NPs) was obtained from Skyspring Nanomaterials, Inc. (Houston, USA). The NPs as reported by the manufacturer are nearly sphere in shape, the average particle size in the range between 10 and 30 nm, and 99.8 % purity. Most chemicals and reagents used in this study were obtained from Sigma, Egypt. Kits for measuring the activity of reduced glutathione (GSH), glutathione-S-transferase (GST), and glutathione reductase (GR) were purchased from Biodiagnostic Co. (Giza, Egypt).

### Experimental Animals

Fifty adult male New Zealand white rabbits with an average age of 9 week-old, weighing between (2.1 and 2.4 kg each) were obtained from the Military Animal Farm (Nasr City, Cairo, Egypt). The rabbits were housed individually in steel cages and provided a 12 hrs light/dark cycle. Temperatures were maintained between 18°C and 26°C, and relative humidity between 30% and 70%. They were fed a commercial diet with free access to water throughout all the experiments.

The rabbits were randomly divided into four groups. Group I (n=5) served as control, whereas groups II, III and IV (n=15 each) were used for the assessment of 0.5, 1.0 and 2.0 % TiO<sub>2</sub>-NPs, respectively. The treatment groups (II, III and IV) were further divided into three sub-groups, each containing five animals and was used for the assessment of one of the experimental time periods (24, 48 and 72hrs). One day before applying the test materials, an area of 4x6cm was clipped in the dorsal back of each rabbit using electric clipper supplied with 0.22mm finishing clipper blade to carefully remove the hair without damaging the skin.

### Preparation of Nanoparticles and Treatment

TiO<sub>2</sub>-NPs was prepared as aqueous suspensions of three concentrations for each (0.5%, 1.0% and 2.0% w/v "percent weight per volume"). Thus, 1.0% aqueous solution of powder in water was made by taking one gram of the powder and dissolving it in distilled water up to 100 ml. The powder first wetted with some de-ionized water, shaken gently to make sure the liquid is making contact with the entire solid.

Then it was diluted to the suitable concentration. The aqueous suspension then ultrasonicated using ultrasonic device (Misonix4000) for 20 to 30min to avoid agglomeration and to ensure the equitable distribution of the particles.

The suspensions were applied topically (2ml) on the shaved areas of the rabbits according to grouping, then covered with pure cotton patch and fixed with non adhesive tape. After each exposure time (24, 48 and 72hrs) the rabbits in each corresponding sub-groups were sacrificed and the shaved areas of skin were quickly removed.

Each specimen was divided into three parts; the 1<sup>st</sup> part was fixed in 10% neutral buffered formalin for the light microscope studies, the 2<sup>nd</sup> part was fixed in 2.5% glutaraldehyde solution in 0.2M phosphate buffer for electron microscope studies and the 3<sup>rd</sup> part was frozen in liquid nitrogen for the molecular studies.

### **Nanoparticles (NPs) Characterization**

#### **Scanning Electron Microscope Analysis**

Thin film of TiO<sub>2</sub>-NPs was prepared on a carbon coated copper grid by just dropping very small amount of the sample on the grid. The grid was allowed to dry for evaporating any undesired solutions or vapors by putting it under a mercury lamp for 5minutes. The samples were analyzed by the SEM using "In-Beam Detector" for high resolution imaging. Images were taken under low accelerating voltages ranging from 15 to 25kV using MIRA3 (TESCAN, Czech Republic) software controlled SEM integrated with Energy Diffraction X-ray spectrum (EDX) system.

#### **X-ray Fluorescence Analysis**

XRF analysis was done using S2 RANGER (Bruker, GmbH, Germany) energy dispersive X-ray fluorescence (EDXRF) spectrometer. The TiO<sub>2</sub>-NPs was placed in aluminum beads to get pressed pellets using press machine.

The elemental analysis was done automatically at 50 Watt power. The obtained Spectrum qualitative multi-element was analyzed via "EQUA ALL" software using multi-element standards in XRF library. The data processing and quantitative results were obtained at the same time with the standard X-Flash software.

#### **The Histological Studies**

#### **The Clinical Manifestations**

Each animal was observed for the recording of clinical signs. The examinations comprised; skin appearance (erythema, edema and lesions), activity, coordination of motion (paralysis, spasms) and breathing.

#### **The Light Microscopy**

For light microscopic study (LM): Formalin (10%) fixed skin slices were processed to form paraffin blocks. Serial sections 5µm in thickness were

prepared and subjected to Haematoxylin and Eosin stain (H&E).

#### **The Electron Microscopy**

For transmission electron microscopic study (TEM): Phosphate buffered glutaraldehyde fixed small pieces of the thin skin were processed to form capsules. Semi-thin sections were cut at 1µm in thickness using glass knife, stained by 1.0 % toluidine blue in 1.0 % borax and examined by light microscope. Ultra-thin sections (50-60nm thickness) were cut using ultra microtome. Then sections were mounted on copper grids and stained with saturated solution of uranyl acetate followed by lead citrate. Ultrathin sections were examined and photographed by JEM-1200 EXII transmission electron microscope in Faculty of Science, Ain Shams University.

#### **The Morphometric and Statistical Analysis**

The epidermal thickness (the distance between the basement membrane and the apical surface of the uppermost nucleated keratinocytes) was measured in H&E stained sections at a magnification of 40X. These measurements were done using photomicrographs that were taken using the light microscope model "Motic DMPL5 with V2 camera" provided with "Motic Prow Plus 2.0 image analysis software" at the Military Technical Research Center. This was performed in three random fields per animal with two reading measurements in each field of all the experiment animals.

All data were expressed as mean (X) ± standard deviation (SD). The analyses were performed by comparing the mean of the control with the mean of each treatment within the three groups using the One Way Analysis of Variance (One Way ANOVA) with Post hoc analysis. Values of  $P < 0.05$  were considered statistically significant. All statistical analysis was performed using the "Graph Pad Prism" version 6.0 software (Graph Pad Software Inc., San Diego, CA, USA).

#### **The Molecular and Biochemical Genetic Studies**

#### **The Glutathione Enzymes**

0.5 gm of skin tissue from each experimental animal was perfuse with 1ml PBS solution containing 0.16 mg heparin to remove any blood cells. The tissue was then homogenized with 5mL cold 100mM potassium phosphate containing 2mM EDTA using "POLYTRON PT 3100 D" electric tissue homogenizer. Samples were centrifuged at 4000 rpm for 20 min at 4°C, and then the supernatant was collected and frozen at - 80°C till assayed.

Glutathione- S- Transferase (GST) activity was assayed according to Habig *et al.* (1974), using (GR-2519) colorimetric assay kit from Biodiagnostic Co. Giza, Egypt following the manufacture procedures. The absorbance of sample (A sample) was measured against the blank at 340 nm. Glutathione Reduced

(GSH) Level was assayed according to Beutler *et al.* (1963), using (GR-2511) colorimetric assay kit from Biodiagnostic Co. Giza, Egypt following the manufacture procedures. The absorbance were measured after 5-10 min at 405 nm of sample (A sample) against the blank using Spectrophotometer Model (Nano Drop 8000/ Thermo scientific Co.). Glutathione Reductase (GR) activity was assayed according to Goldberg and Spooner (1983), using (GR-2523) assay kit from Biodiagnostic Co. Giza, Egypt following the manufacture procedures. The initial absorbance was measured against air at 340 nm, then time started simultaneously and reads were taken after 1 min for a period of 5 min to obtain the change in absorbance ( $\Delta A_{340}$  nm/ min)

### Esterases and Protein Electrophoresis

One gm of each sample was grind with 2 ml (0.1 M Tris-borate-EDTA buffer, pH 8.9) grinding solution using electric tissue homogenizer with controlled velocity for about 15 strokes of the rod in the grinding tube for 1 min under cooling.

The homogenate was frozen and thawed, then centrifuged at 12,000 rpm, for 30 min at 4 °C, in "Martin Christ II" refrigerated centrifuge. The supernatant was isolated and re-centrifuged for another 30 min under the same conditions. A portion of the clear supernatant of each sample was diluted in 1:1 ratio with the sample buffer to be used for electrophoresis.

nonspecific esterases were electrophoretically separated from the skin tissue of rabbits by using the Native Polyacrylamide Gel Electrophoresis (N-PAGE) technique using  $\alpha$  - Naphthyl acetate as substrate according to the method of Davis (1964) under non-denatured conditions (10 % separating gel and 4 % stacking gel). Electrophoresis was conducted at a constant 200 V/10-200mA (100 V per gel) for 4 hrs inside (4 °C) cold chamber.

The general proteins were separated from the skin by using the SDS Polyacrylamide Gel Electrophoresis (SDS-PAGE) technique according to Laemmli (1970). The proteins SDS-PAGE was performed in a vertical electrophoresis unit "XCell4 Sure Lock Midi-Cell", 13 x 8.3 cm / 1 mm thickness, (Life Technologies), under denatured conditions. The gels were covered with staining solution contains 0.2 % Coomassie brilliant blue R-250 in a mixture of methanol, dH<sub>2</sub>O and acetic acid (45:45:10) in plastic box, and left overnight on shaker at room temperature.

## 3- Results

### The Nanoparticles (NPs) Characterization Scanning Electron Microscope (SEM)

SEM examinations revealed that, TiO<sub>2</sub>-NPs was singly distributed. Aggregates of small clusters were rarely seen. The morphological structure of TiO<sub>2</sub>-NPs

was assessed as spherical NPs with smooth and clear surface. Based on the simultaneous measurements of the single NPs by SEM, the calculated mean diameter of TiO<sub>2</sub>-NPs was 25.4 ± 0.3 nm (Fig. 1).

The EDX analysis confirmed the presence of the main component elements in the examined TiO<sub>2</sub>-NPs samples, Titanium (Ti) and Oxygen (O) were present. in addition, the analysis revealed the presence of Carbon (C) element. This is due to the substrate over which they were held on the grids to perform the SEM characterization (Fig. 2).

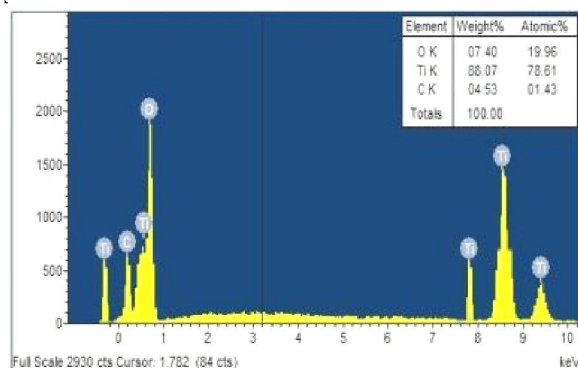
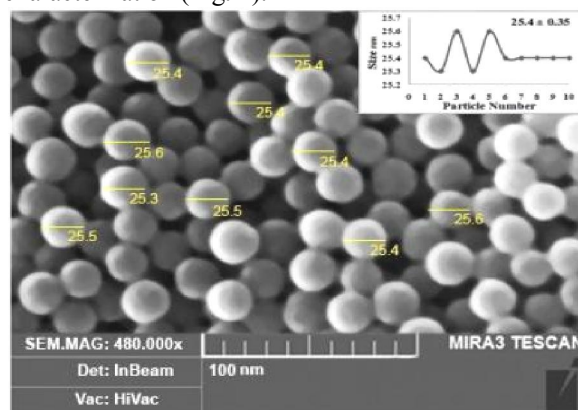


Figure (2): The EDX spectrum of TiO<sub>2</sub>-NPs showing the elemental composition.

### X-Ray Fluorescence (XRF)

The XRF analysis result of TiO<sub>2</sub>-NPs revealed 99.7 % purity of TiO<sub>2</sub>. Other impurities such as Na<sub>2</sub>O, SiO<sub>2</sub>, MgO, Al<sub>2</sub>O<sub>3</sub>, Nb<sub>2</sub>O<sub>5</sub>, P<sub>2</sub>O<sub>5</sub>, K<sub>2</sub>O and Fe<sub>2</sub>O<sub>3</sub> were detected in the samples (Table. 1).

Table (1): The result of XRF analysis of TiO<sub>2</sub>-NPs

Element	Weight %	Element	Weight %
TiO <sub>2</sub>	99.7	Nb <sub>2</sub> O <sub>5</sub>	0.031
Na <sub>2</sub> O	0.036	P <sub>2</sub> O <sub>5</sub>	0.043
SiO <sub>2</sub>	0.016	K <sub>2</sub> O	0.034
MgO	0.014	Fe <sub>2</sub> O <sub>3</sub>	0.052
Al <sub>2</sub> O <sub>3</sub>	0.074	Sum	100 %

## The Histological and Ultrastructure Studies

### Group I (the control group)

Clinical manifestation of the control rabbits revealed a good sanitary status, where the macroscopic examinations showed healthy skin with no lesions, erythema or edemas. Normal activities and behaviors were recorded with coordination of motion, and no signs of spasm. All the control rabbits showed similar basic features of skin by light and electron microscopes examination.

Light microscopic examination of H&E-stained sections and semithin sections of the skin of rabbits showed normal histological architecture with the characteristic epidermis and dermis.

The epidermis, which forms the uppermost multilayered compartment of the skin, consisted of stratified squamous keratinized epithelium formed mainly of keratinocytes. These cells were arranged according to their position and morphology into four layers as shown in Figs.3 and 4:

- The stratum corneum, the superficial non-cellular horny layer, consisted of many layers of flattened non-nucleated acidophilic keratinized cells.

- The stratum granulosum consisted of spindle shaped flattened cells whose cytoplasm appeared to contain abundant basophilic keratohyalin granules.

- The stratum spinosum layer consisted of a variety of cells that differed in shape depending on their location. Supra-basal cells were polygonal in shape with central vesicular nuclei, whereas cells of the upper spinosum were generally larger in size, but flattened with smaller nuclei.

- The basal layer of keratinocytes, associated with the basal lamina, was found to be formed of a single layer of low basophilic columnar cells with oval to rounded dark stained nuclei.

The dermis showed irregular twisted surfaces, with dermal papillae interdigitated with epidermal ridges. It had rich network of blood vessels and hair follicles, with associated sebaceous glands.

Electron microscopic examination of the skin of the control group showed normal structure of the epidermis and dermis. The epidermis had four layers of keratinocytes:

- The stratum corneum layer was thin and composed of well organized flattened horny dead cells (corneocytes). These cells contained no nuclei or cytoplasmic organelles, but were filled with keratin filaments embedded in an amorphous matrix. The lower layers of SC were closely attached to the stratum granulosum, while the outer layers appeared loosen and fully keratinized (Fig. 5).

- The cells of stratum granulosum appeared spindle in shape with elongated nucleus. Their cytoplasm was filled with small keratohyalin granules,

and surrounded by few bundles of intermediate keratin filaments (Fig. 6).

- The cells of stratum spinosum had large rounded to oval nuclei, with apparent nucleoli. Their cytoplasm showed well-organized bundles of intermediate filaments (tonofilaments) that were condensed at the sites of desmosomes. Several rounded mitochondria were also located (Fig. 7).

- The basal cells were columnar in shape with oval to rounded nuclei. These nuclei possessed extended euchromatin and apparent nucleoli. The cells were resting on a basal lamina, where network of keratin intermediate filaments were condensed to form hemidesmosomes along the dermal-epidermal junction that connecting the basal layer cells with the basement membrane. The cytoplasm contained several oval to rounded mitochondria, besides other types of cell organelles. These cells were connected together as well as with the adjacent cells and with the super basal cells by desmosomal junctions (Fig. 8).

The dermis showed normal collagen fibers. The hair appeared with its typical normal structure. Its inner and outer root sheaths were surrounded by hair dermal sheath of organized connective tissue, while the associated sebaceous gland cells appeared with the characteristic fat droplets in their cytoplasm.

### Group II (0.5 % TiO<sub>2</sub>-NPs treatment)

Macroscopic examination of the skin of rabbits after treatments with 0.5% TiO<sub>2</sub>-NPs for 24, 48 and 72 time periods revealed normal skin appearance, as well as, no changes in the activities and behaviors of rabbits were noted.

At the end of the three exposure times (24, 48 and 72 hrs), the light microscopic examination of the treated skin of this sub-group showed normal histological structure with nearly no remarkable difference as compared to control.

### Group III (1.0 % TiO<sub>2</sub>-NPs treatment)

Macroscopic examination and clinical manifestation did not reveal any clinical signs of the influence of 1.0 % TiO<sub>2</sub>-NPs on the skin appearance after 24 and 48 exposure times. In addition, no abnormal activities or behaviors were noted on the treated rabbits.

Examination of skin sections of this sub-group with light microscope also showed normal histological structure with nearly no remarkable changes after 24 and 48hrs exposure times.

#### 3.1. After 72 hours exposure

Macroscopic examination of the skin of rabbits after 72 hrs exposure to 1.0 % TiO<sub>2</sub>-NPs showed well defined erythematous patches and moderate edemas, however, no lesions or scars were distinguished.

LM examination of skin specimens from the treated skin with 1.0 % TiO<sub>2</sub>-NPs for 72hrs revealed several structural changes (Figs. 9, 10):

- The thickness of stratum corneum layer was increased (hyperkeratosis).

- Few detachments between stratum granulosum and stratum corneum were noted in some sections.

- Slight decrease in the thickness of the viable epidermis with disorganization of the keratinocytes in all layers.

- Increase of the intercellular spaces between the keratinocytes was dominant, with the occurrence of numerous cells with moderately pyknotic nuclei.

- Intercellular edema was noted through the lower epidermal layers especially in the spinosum one.

- The dermis appeared with normal morphology.

Electron microscopic examinations revealed the following ultrastructure changes:

- The stratum corneum layer became very thick and more compact with the thinning of the individual keratin layers. Separations from the next granular layer were evident by the presence of many vacuolated areas (Fig. 11).

- The stratum granulosum layer appeared thinner and contained large amount of keratohyalin granules as compared with the control. Large vacuolization was noted in many areas detaching the granular layer from the horny layer. Some granular cells showed nuclear karyolysis, others showed degeneration of cytoplasmic contents, as they appeared electron lucent (Fig. 12).

- The stratum spinosum layer showed degenerative changes, where some cells became distorted and shrunken with irregular or fragmented nuclei surrounded by vacuolated cytoplasm. Noticeable increase of the intercellular spaces and disruption or losses of desmosomal junctions were also noted. Other cells apparent signs of necrosis such as the ruptured nuclear and/or cellular membranes, swollen and rupture mitochondria (Fig. 13).

- The basal layer cells showed minor structural alterations, where some cells appeared flattened with elongated nuclei and irregular nuclear membrane. Vacuolated cytoplasm, swollen mitochondria and few distributed hemidesmosomes along the dermal-epidermal junction were also noted and the basal lamina was maintained normally separating the epidermis from dermis (Fig. 14).

- The dermis appeared with normal morphology.

#### **Group IV (2.0 % TiO<sub>2</sub>-NPs treatment)**

##### **After 24 hours exposure**

By macroscopic examination, no abnormal symptoms on the skin appearance could be distinguished after the topical application of 2.0 % TiO<sub>2</sub>-NPs for 24hrs.

Moreover, LM examinations of the skin showed normal histological structure. Hence, no alterations were seen throughout the four epidermal layers, and the entire dermis.

##### **After 48 hours exposure**

Macroscopic examination of the rabbits treated with 2.0 % TiO<sub>2</sub>-NPs for 48hrs revealed slight edema, moderate erythema and scaly appearance of the skin surface.

LM examinations revealed a number of structural changes (Figs. 15, 16):

- The granulosum layer showed an increase in its thickness, with a noticeable excess in the amount of large dark keratohyalin granules.

- The spinosum layer became thin and some of the keratinocytes appeared shrunken with the widening of intercellular spaces and separation of cells. Some cells showed deeply stained pyknotic nuclei surrounded by pale clear vacuolated cytoplasm, and others showed karyolytic nuclei.

- The basal layer contained cells with pyknotic and karyolytic nuclei.

- The basal lamina was still visible separating the dermis from the epidermis along the dermal-epidermal junction, and dermis was structurally normal.

Electron microscopic examination revealed the following ultrastructure changes:

- The stratum corneum layer appeared with its normal thickness and organization as compared with the control. However, a few vacuolated detachments from the granulosum layer were noted. The stratum granulosum layer showed an increase in thickness, and the cells were loaded with large clumps of keratohyalin granules (Fig. 17).

- The basal and spinosum layers became abnormal where some cells showed large cytoplasmic vacuoles (intracellular edema). Others appeared with electron-dense cytoplasm that contained dense bodies and swollen mitochondria with disrupted cristae. Irregular tonofilaments distribution was observed inside some keratinocytes, as well as partial loss of the desmosomes with widening of the intercellular spaces (Figs. 18, 19). Moreover, some supra basal cells showed marked signs of necrosis with nuclear and cellular membranes rupture, and cytoplasm filled by many swollen mitochondria (Figs. 19, 20). The basal lamina was well defined with normal hemidesmosomes and the dermis appeared with no changes (Fig. 20).

##### **After 72 hours exposure**

Macroscopic examination of the skin of rabbits after 72hrs exposure to 2.0 % TiO<sub>2</sub>-NPs showed well defined red patches which may regarded as severe erythema. Besides, moderate edema and slight scars formations were distinguished. The rabbits became nervous with obvious jumpy movement accompanied by fast breathing and a tendency to excessive drinking.

LM examination of the treated skin (TiO<sub>2</sub>-NPs 2.0 % / 72hrs) revealed a number of structural changes (Figs. 21, 22):

- Hyperkeratosis of stratum corneum layer with the decrease in the thickness of the granulosum layer.

- The keratinocytes of the spinosum layer became shrunk, rounded, and contained eosinophilic cytoplasm. In addition, lose of the intercellular bridges between the peripheral keratinocytes, and increase the intercellular spaces were noted. Moreover, the nuclei of some cells appeared dark and small (pyknotic), whereas other nuclei appeared more electron lucent (karyolytic).

- Some cells of the stratum basal showed vacuolization and some appeared shrunken with deformed nuclei (necrotic), whereas, others showed normal appearance.

- Breaks in the basement membrane were obviously noted, and the dermis appeared vacuolated with aggregation of lymphocytes.

Electron microscopic examinations revealed devastating ultrastructure changes:

- The stratum corneum layer showed hyperkeratosis, with incomplete keratinization of corneocytes, where nuclei remained in the cells (parakeratosis). In addition, the stratum corneum cells showed disorganization, protrusion, loss of normal regular lamellae, and the appearance of numerous spaces separating the keratin layers (Fig. 23).

- The stratum granulosum layer appeared thin with signs of granular degeneration, where numerous vacuolated cells containing large keratohyalin granules appeared with a marked decrease in fibrillar contents. The cytoplasm became more electron lucent with cellular vacuolization. The stratum spinosum keratinocytes showed various stages of degeneration as the chromatin texture disappeared and the nuclear membrane was disrupted or absent. Degenerated mitochondria, lysosomal vacuoles and marked decrease in tonofilaments content with disruption of desmosomes and intercellular disjunctions, widening in the intercellular separations and folds with void areas in place of intercellular contacts were also seen. All these features indicate the occurrence of necrosis (Fig. 24).

- The basal layer cells showed more electron-dense cytoplasm, swollen mitochondria and dark sparse tonofilaments. The nuclei of these cells showed an irregular nuclear membrane and increased peripheral chromatin. Increased intercellular spaces, damage hemidesmosomes, loosen intermediate filaments, and broken connection between the basal layer of the epidermis and the underlying dermal matrix were also recorded. The basal lamina appeared discontinuous, broken, and lost its regular appearance (Fig. 25).

- In the dermis, disorganized closely packaged thick collagen fibers, numerous vacuolated areas and

many fibroblasts that contained swollen and degenerated mitochondria were observed (Fig. 26).

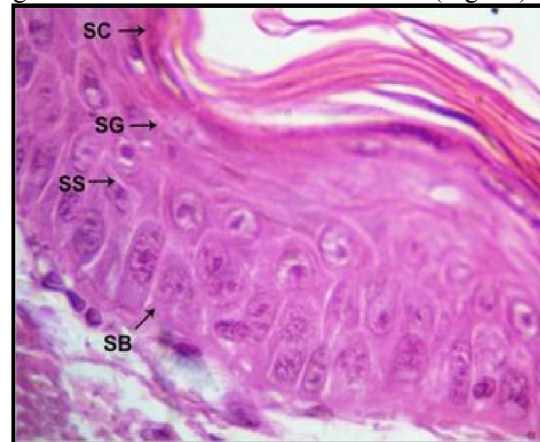


Figure (3): Photomicrograph of section of a skin of the control group showing the epidermal layers. (100 x, H&E)

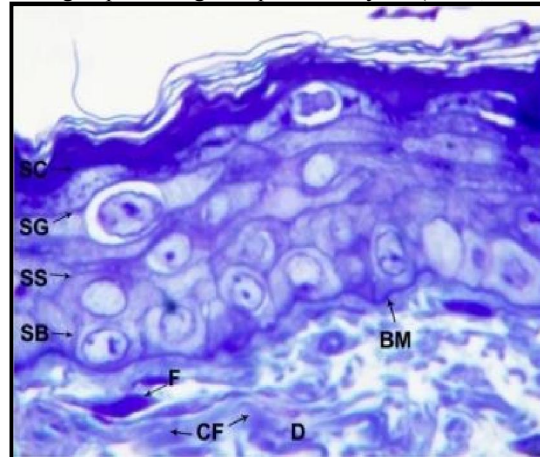


Figure (4): Photomicrograph of semithin section of skin of the control group showing the four epidermal layers, the basal lamina. The dermis (D) showing many fibroblasts (F) and well organized collagen fibers (CF). (100 x; toluidin blue).

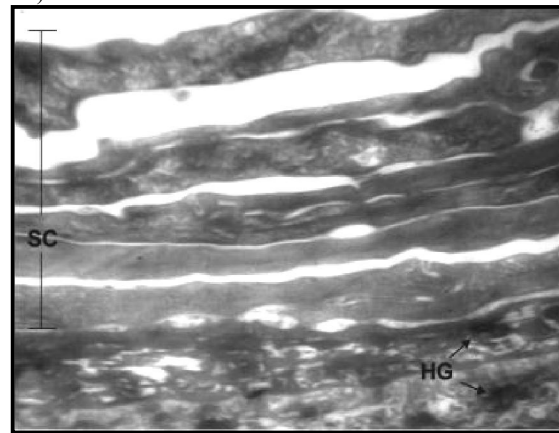


Figure (5): Electron micrograph of the upper portion of the epidermis of a control skin showing thin compact stratum corneum (SC) layer with well organized dead un-nucleated corneocytes. (10000x)

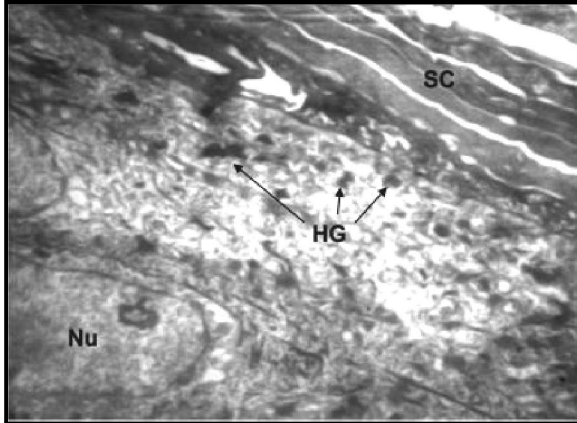


Figure (6): Electron micrograph of a control skin showing thin compact stratum granulosum (SG) layer with its spindle-shaped cells, elongated nucleus (Nu) and keratohyalin granules (HG).(10000x).



Figure (9): Photomicrograph of section of group III treated skin (TiO<sub>2</sub>-NPs 1.0 % / 72hrs) revealing hyperkeratosis of stratum corneum. Notice the intercellular edema (blue arrows), increase intercellular separations (green arrows), and pyknotic cells (yellow arrows).(100 x, H&E).

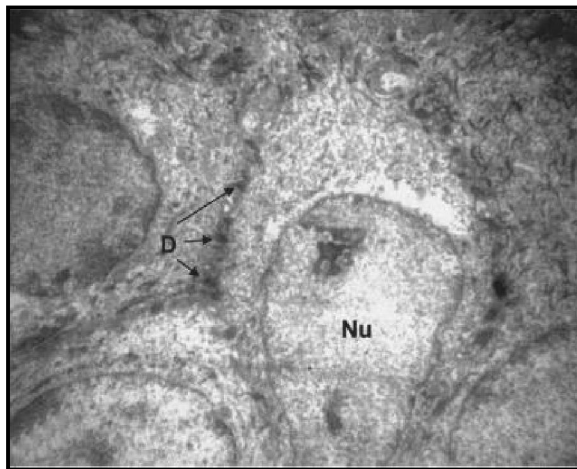


Figure (7): Electron micrograph showing a part of the stratum spinosum layer of a control skin. These cells are attached together by desmosomes (D).(3000x).

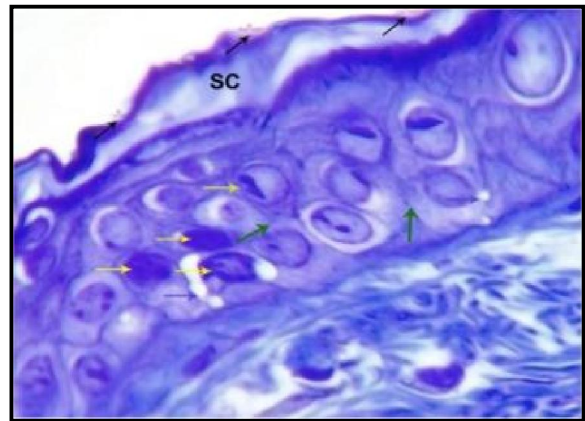


Figure (10): Photomicrograph of semithin section of a group III treated skin (TiO<sub>2</sub>-NPs 1.0 % / 72hrs) showing intercellular edema (blue arrows), increased intercellular spaces (green arrows), and pyknotic cells (yellow arrows). Notice the aggregation of NPs (black arrows). (100x, toluidin blue).

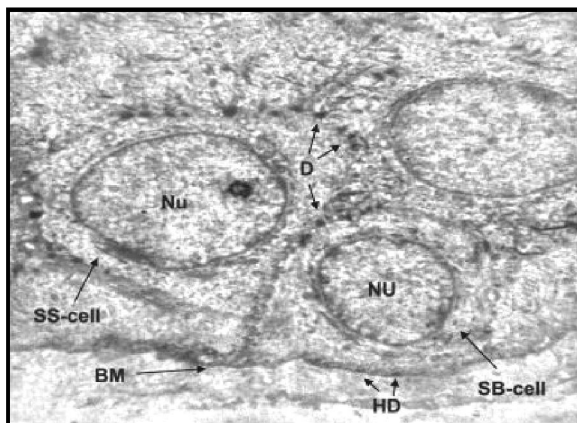


Figure (8): Electron micrograph of a control skin showing stratum basal (SB) cells. These cells are attached to the basal lamina (BM) by many hemidesmosomes (HD) and to the adjacent cells by desmosomes (D). (10000x).

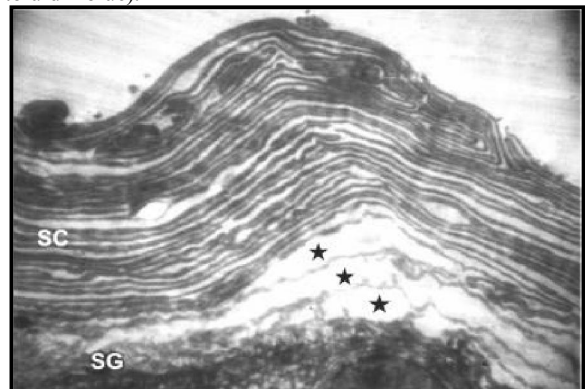


Figure (11): Electron micrograph of the upper epidermis of a group III treated skin (TiO<sub>2</sub>-NPs 1.0 % / 72h) showing hyperkeratosis of stratum corneum layer (SC), and the highly vacuolated detachment from the stratum granulosum layer (stars).(2000x).

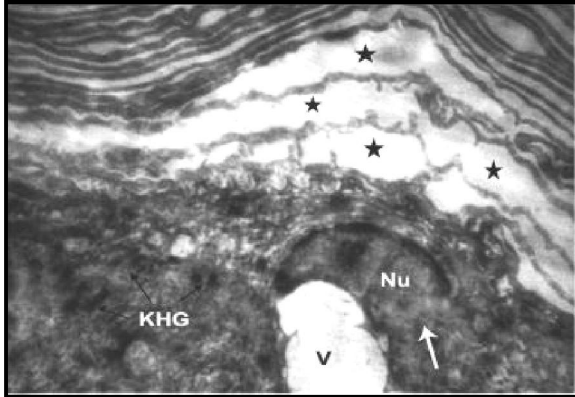


Figure (12): Electron micrograph of a group III treated skin ( $\text{TiO}_2\text{-NPs}$  1.0 % / 72h) showing granular cell with ruptured nuclear membrane (white arrow), large cytoplasmic vacuolization (V), and excessive keratohyalin granules (KHG). Notice the detachment of horny layer (black star). (3000 x).

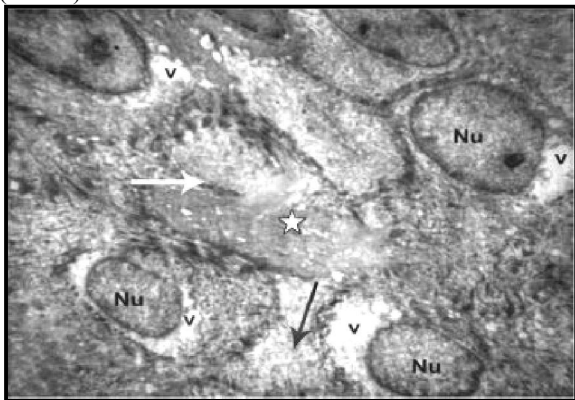


Figure (13): Electron micrograph of a part of the epidermis of a group III treated skin ( $\text{TiO}_2\text{-NPs}$  1.0 % / 72hrs) showing stratum spinosum layer containing degraded cell (white arrow), with membranes rupture (star). Notice the vacuolated cytoplasm (V), and wide intercellular separations (black arrow). (2000x).

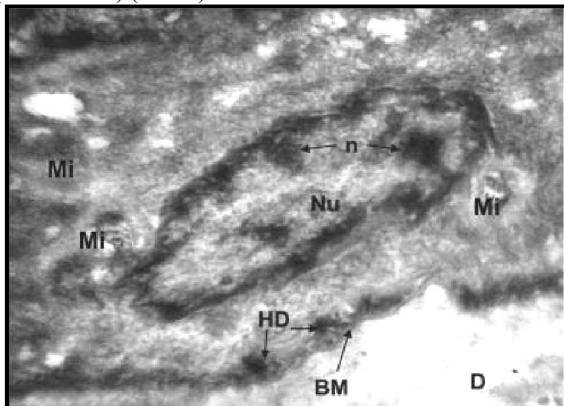


Figure (14): Electron micrograph of a group III treated skin ( $\text{TiO}_2\text{-NPs}$  1.0 % / 72hrs) showing abnormal basal layer cell with fragmented nucleoli (n), swollen mitochondria (Mi). The basal lamina (BM) was still normal and associated with few hemidesmosomes (HD). (6000x).

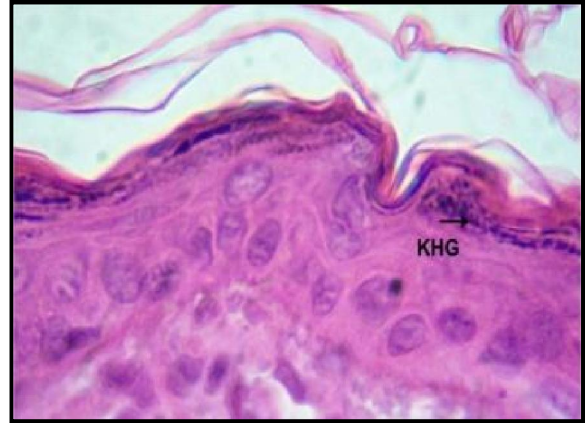


Figure (15): Photomicrograph section from a group IV treated skin ( $\text{TiO}_2\text{-NPs}$  2.0 % / 48hrs) showing an increase in the thickness of the granular layer with excessive amount of large keratohyalin granules (KHG). (100 x, H&E).

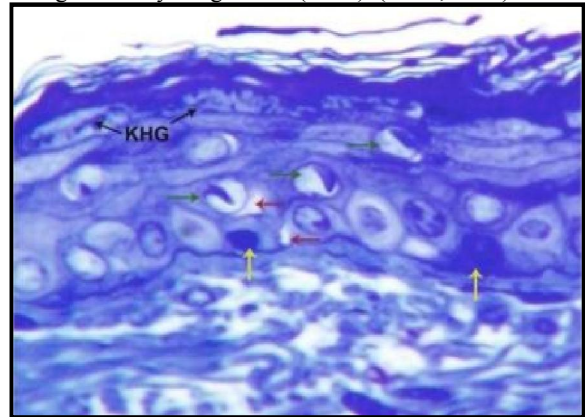


Figure (16): Photomicrograph of semithin section from a group IV treated skin ( $\text{TiO}_2\text{-NPs}$  2.0 % / 48hrs) showing pyknotic cells (green arrows), necrotic cells (yellow arrow), intercellular edema (red arrows) and excessive keratohyalin granules (KHG) in the granular layer. (100 x, toluidin blue).

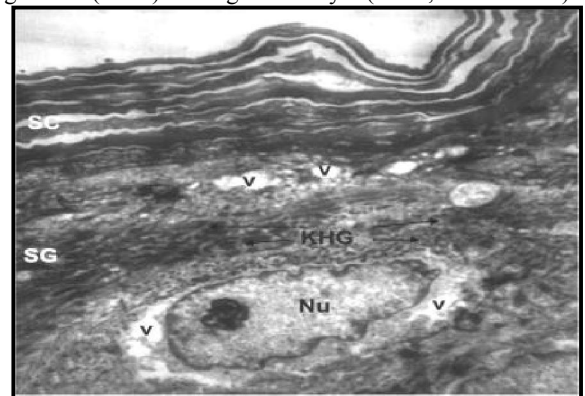


Figure (17): Electron micrograph of a part of the upper epidermis of a group IV treated skin ( $\text{TiO}_2\text{-NPs}$  2.0 % / 48hrs) showing the stratum corneum layer (SC) with normal thickness and organization of corneocytes. This micrograph also reveals the presence of vacuoles (V) and stratum granulosum detachment (SG). (3000x).

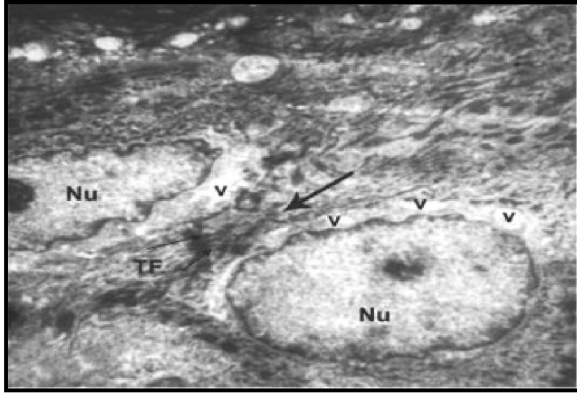


Figure (18): Electron micrograph of the upper epidermis of a group IV treated skin (TiO<sub>2</sub>-NPs 2.0 % / 48hrs) showing stratum spinosum cell with large indented nuclei (Nu) surrounded by vacuolated cytoplasm (V), vast intercellular separations (arrow), and clumping of tonofilaments (TF).(3000x).

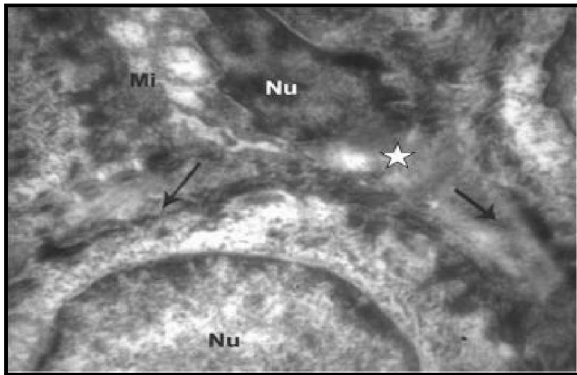


Figure (19): Electron micrograph of part of lower epidermis of a group IV treated skin (TiO<sub>2</sub>-NPs 2.0 % / 48hrs) revealing a supra basal cell necrosis as evident by the presence of pyknotic nuclei, ruptured membranes (star), swollen mitochondria (Mi) and the loss of desmosomal junction (arrows).(8000x).

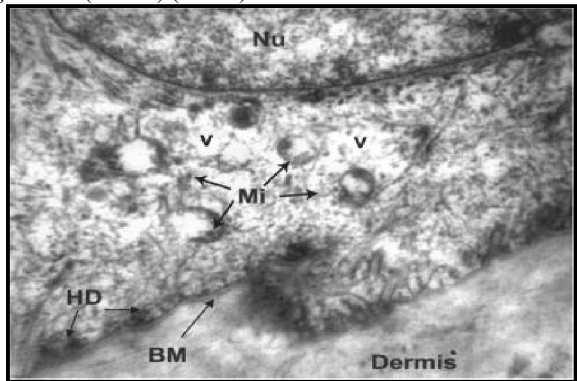


Figure (20): High magnification electron micrograph showing a part of a basal layer cell of the epidermis of a group IV treated skin (TiO<sub>2</sub>-NPs 2.0 % / 48hrs). The cytoplasm appears vacuolated (V) with many swollen and ruptured mitochondria (Mi). The basement membrane (BM) is still visible with few hemidesmosomes (HD).(10000x).

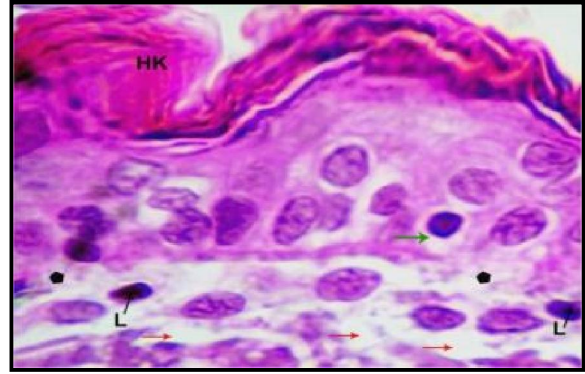


Figure (21): Photomicrograph of section from a group IV treated skin (TiO<sub>2</sub>-NPs 2.0 % / 72hrs) showing hyperkeratosis of the horny layer (HK), necrotic cell in basal layer (green arrow) with breaking of the basal lamina (pentagonal). Notice the vacuolization of the dermis (red arrow), and invasion of lymphocytes (L). (100 x, H&E).

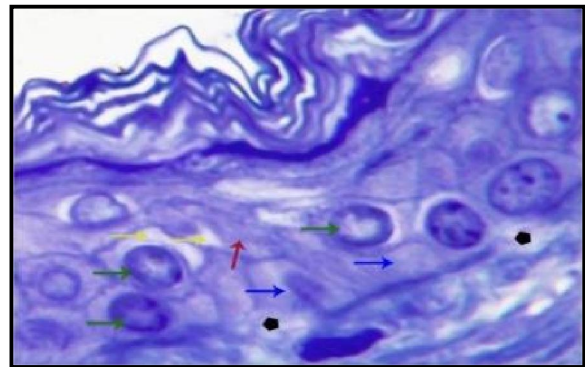


Figure (22): Photomicrograph of semithin section from a group IV treated skin (TiO<sub>2</sub>-NPs 2.0 % / 72hrs) showing hyperkeratosis. Spinosum cells with fragmented nuclei (green arrows). Others appeared degenerated (red arrow). Notice the intercellular edema (yellow arrows), deformation of basal cells (blue arrows) and breaking of the basal lamina (pentagonal). (100 x, toluidin blue).

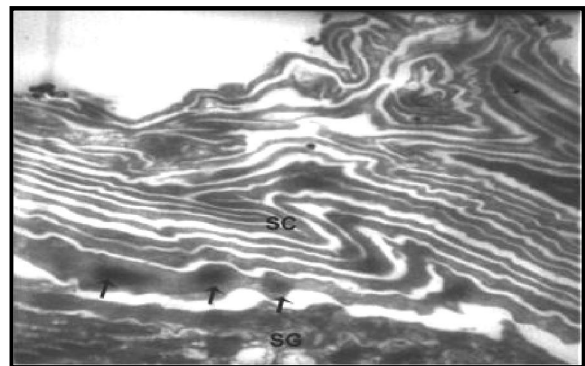


Figure (23): Electron micrograph of a group IV treated skin (TiO<sub>2</sub>-NPs 2.0 % / 72hrs) showing hyperkeratosis of the stratum corneum (SC) layer. Notice the remarkable parakeratosis where nuclei remained in the cells (arrows).(3000x)

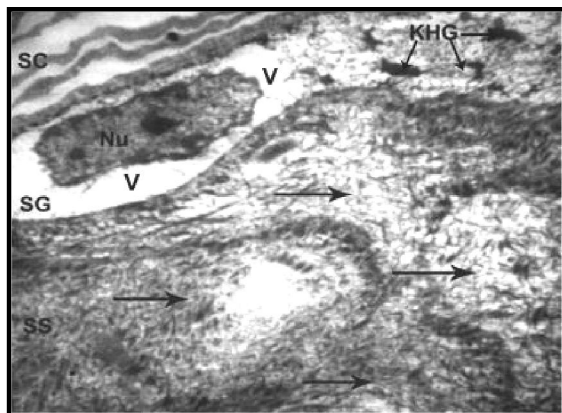


Figure (24): Electron micrograph of a group IV treated skin ( $\text{TiO}_2\text{-NPs}$  2.0 % / 72hrs) revealing abnormal stratum granulosum cell (SG) with deformed nucleus (Nu), vacuolated cytoplasm (V) and containing large keratohyalin granules (KHG). Notice the degeneration of the stratum spinosum cells (black arrows). (2000x).

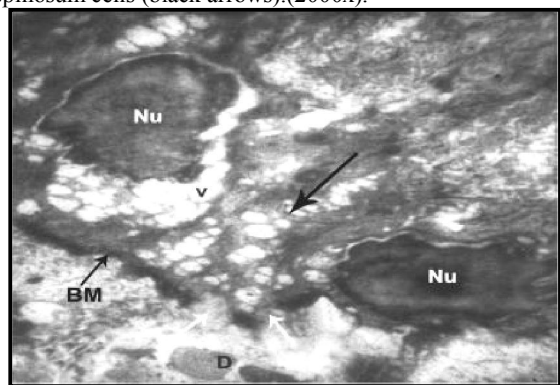


Figure (25): Electron micrograph of a group IV treated skin ( $\text{TiO}_2\text{-NPs}$  2.0% / 72hrs) revealing a broken basal lamina (white arrows) and loss of hemidesmosomes. Notice the abnormal basal cell in the upper left with deformed nucleus (Nu), vacuolated cytoplasm (V), and wide intercellular spaces (black arrows). (3000x).

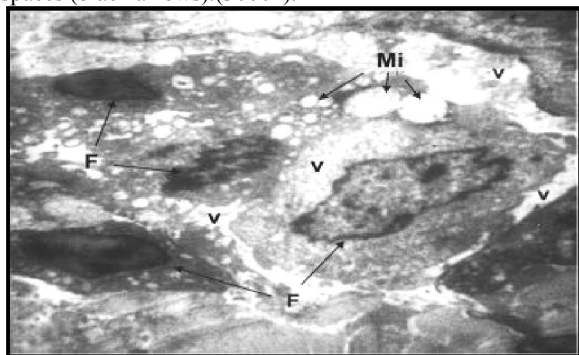


Figure (26): Electron micrograph from a part of dermis of a group IV treated skin ( $\text{TiO}_2\text{-NPs}$  2.0 % / 72hrs) showing numerous vacuoles (V) and fibroblasts (F) contain many swollen and degenerated mitochondria (Mi). (2000x).

### The Morphometric and Statistical Results

Statistical analysis of the morphometric measurements in H&E-stained sections of the skin of

rabbits of  $\text{TiO}_2\text{-NPs}$  treatment are shown in Table 2 and Fig. 27. The mean epidermal thickness of the control (group I) was measured as  $14.16 \pm 0.545 \mu\text{m}$ . This value was used for the statistical analysis, and to assess the variations of the other treated groups.

The 0.5%  $\text{TiO}_2\text{-NPs}$  (group II) treated skin, showed no significant differences in the thickness of nucleated epidermal keratinocytes at the exposure times of 24, 48, and 72hrs ( $P < 0.05$ ).

Also, the skin of rabbits of the group III (1.0 %  $\text{TiO}_2\text{-NPs}$ ) illustrated no significant differences ( $P < 0.05$ ) in the epidermal thickness at the exposure times of 24 and 48hrs. Whereas at 72hrs, the mean epidermal thickness was  $11.23 \pm 0.407 \mu\text{m}$ , with a significant decrease below the control value by 20.7 % at  $P < 0.05$ .

In the group IV treated skin with 2.0 %  $\text{TiO}_2\text{-NPs}$  there was no significant difference in the epidermal thickness from the control ( $P < 0.05$ ) at the exposure time of 24hrs. However, at the 48hrs exposure time, the mean epidermal thickness was  $11.06 \pm 0.359 \mu\text{m}$ , with a significant decrease below the control value by 21.9 % ( $P < 0.05$ ), whereas, at the 72hrs exposure time, there was a highly significant decrease ( $P < 0.05$ ) in the mean thickness of the epidermis ( $10.52 \pm 0.292 \mu\text{m}$ ) from the control value by 25.7%.

### Molecular and Biochemical Genetics Results

#### The Glutathione Enzymes

In the control animals skin extracts (group I), the mean  $\pm$  SD for GST activity expressed as U/g.tissue was  $24.54 \pm 2.61$ , and the activity of GR as expressed in U/L was  $1574.9 \pm 120.03$ , while the concentration of GSH was  $92.27 \pm 3.91 \text{ mg/g.tissue}$ . These values were used for the statistical analysis, and to assess the variations of the other treated sub-groups.

Table (2): Summary of the mean thickness of nucleated epidermal keratinocytes in the skin of rabbits treated with  $\text{TiO}_2\text{-NPs}$  and their relations.

Treatment		Epidermal thickness ( $\mu\text{m}$ )
Control		$14.16 \pm 0.545$
0.5 % $\text{TiO}_2\text{-NPs}$	24 hrs	$14.11 \pm 0.389$
	48 hrs	$14.18 \pm 0.461$
	72 hrs	$14.19 \pm 0.506$
1.0 % $\text{TiO}_2\text{-NPs}$	24 hrs	$14.17 \pm 0.591$
	48 hrs	$14.07 \pm 0.385$
	72 hrs	$11.23 \pm 0.407^*$ ( $\downarrow$ 20.7 %)
2.0 % $\text{TiO}_2\text{-NPs}$	24 hrs	$13.73 \pm 0.380$
	48 hrs	$11.06 \pm 0.359^*$ ( $\downarrow$ 21.9 %)
	72 hrs	$10.52 \pm 0.292^*$ ( $\downarrow$ 25.7 %)
- Each value represents the mean $\pm$ SD		
- (*) Significantly different as compared to control, at $P < 0.05$ .		
- ( $\downarrow$ ) Indicates percent decrease.		

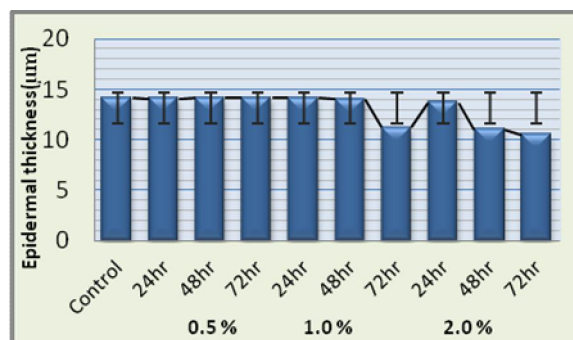


Figure (27): The mean  $\pm$  SD and significant differences ( $P < 0.05$ ) of epidermal thickness in the skin of rabbits treated with TiO<sub>2</sub>-NPs.

The activities of GST and GR enzymes and the concentration of GSH in the skin of rabbits of TiO<sub>2</sub>-NPs treatment groups are shown in Table 3 and Figs. 28, 29 and 30 as mean  $\pm$  SD for the different treatments of TiO<sub>2</sub>-NPs, besides the significant differences as compared to control at  $P < 0.05$ . These differences were expressed in percentage as regarded to the control.

No statistically significant differences were found in the activities of GST and GR or in the

concentration of GSH, after exposure to TiO<sub>2</sub>-NPs at a dose of 0.5 % (group II) for 24, 48, or 72hrs. The GST and GR were increased in the rabbits skin treated with 1.0 % TiO<sub>2</sub>-NPs (group III) for 72hrs over the control value by 33.8 % and 13.5 %, respectively, whereas the GSH was decreased by 24.7 %. The same concentration of TiO<sub>2</sub>-NPs had no influence on the investigated enzymes at 24 and 48hrs exposures time as compared to the control. At the concentration of 2.0 % TiO<sub>2</sub>-NPs (group IV), no significant differences were demonstrated in the enzymatic activities of GST and GR or in the concentration of GSH ( $P < 0.05$ ) after 24hrs.

After 48hrs exposure to the same concentration, the treated skin demonstrated a noticeable increase in the activities of GST and GR over the control value by 20.1 % and 10.4 %, respectively. In contrast, the concentration of GSH reduced by 15.2 %.

Increasing the exposure time to 72hrs increased the enzymatic activities of GST and GR as compared to control. The percentage of the increase was 55.2 % and 42.9 %, respectively. On the other hand, the concentration of GSH was decreased by 29.3 % with respect to the control.

Table (3): The activities of GST and GR, and GSH level in the skin of rabbits after exposure to different treatments of TiO<sub>2</sub>-NPs.

Treatment		GST (U/g. tissue)	GR (U / L)	GSH (mg/g. tissue)
Control		24.54 $\pm$ 2.61	1574.9 $\pm$ 120.03	92.27 $\pm$ 3.91
TiO <sub>2</sub> 0.5%	24 hr	24.50 $\pm$ 2.69	1484.3 $\pm$ 211.41	92.22 $\pm$ 6.40
	48 hr	24.21 $\pm$ 1.91	1603.9 $\pm$ 433.15	91.64 $\pm$ 4.87
	72 hr	24.50 $\pm$ 1.14	1598.8 $\pm$ 203.90	93.12 $\pm$ 4.49
TiO <sub>2</sub> 1.0%	24 hr	24.38 $\pm$ 2.86	1498.5 $\pm$ 424.32	93.08 $\pm$ 4.64
	48 hr	24.60 $\pm$ 2.35	1573.1 $\pm$ 271.69	94.35 $\pm$ 6.04
	72 hr	32.83 $\pm$ 0.97* ( $\uparrow$ 33.8 %)	1787.8 $\pm$ 235.39* ( $\uparrow$ 13.5 %)	69.47 $\pm$ 3.29* ( $\downarrow$ 24.7 %)
TiO <sub>2</sub> 2.0%	24 hr	24.44 $\pm$ 3.31	1573.2 $\pm$ 347.84	92.88 $\pm$ 5.61
	48 hr	29.48 $\pm$ 1.48* ( $\uparrow$ 20.1 %)	1737.6 $\pm$ 126.21* ( $\uparrow$ 10.4 %)	78.22 $\pm$ 2.20* ( $\downarrow$ 15.2 %)
	72 hr	38.09 $\pm$ 1.77* ( $\uparrow$ 55.2 %)	2250.7 $\pm$ 274.94* ( $\uparrow$ 42.9 %)	65.24 $\pm$ 2.16* ( $\downarrow$ 29.3 %)

- Each value represents the mean  $\pm$  SD of five rabbits (triplicate reading of each).

- (\*) Significantly different as compared to control, at  $P < 0.05$ .

- ( $\uparrow$ ) Indicates percent increase.

- ( $\downarrow$ ) Indicates percent decrease.

### Nonspecific Esterases (Est.) Electrophoresis

The electrophoretic pattern for nonspecific esterases of the skin of rabbits treated with different concentrations of TiO<sub>2</sub>-NPs is shown in Fig. 31. A total of eight esterase bands were recognized in the skin extracts, with Relative mobility (Rm) values ranging from 0.49 to 0.94. The bands were numbered sequentially according to their position in the gel, and to their Rm values toward the anode (Fig. 31). To facilitate the assessment of variations among esterase bands an electropherogram was designed on the bases

of the sites of esterase, activity, band intensity and the relative mobility (Fig. 32).

The eight bands were distributed into two moderately spaced zones; A and B according to their anodic migration. Zone (A) includes the first three esterase bands (A1, A2 and A3) while, zone (B) contains the remaining five bands (B1, B1Ti, B2, B3 and B4Ti). Band number A1 is the most cathodic one with 0.49 Rm, whereas, B4Ti is the most anodic one with 0.94 Rm (Fig. 32).

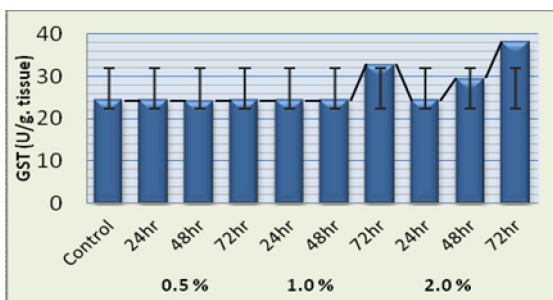


Figure (28): The mean  $\pm$  SD and significant differences ( $P < 0.05$ ) of GST activity in the skin of rabbits treated with TiO<sub>2</sub>-NPs.

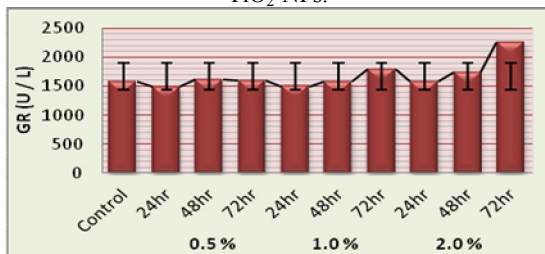


Figure (29): The mean  $\pm$  SD and significant differences ( $P < 0.05$ ) of GR activity in the skin of rabbits treated with TiO<sub>2</sub>-NPs.

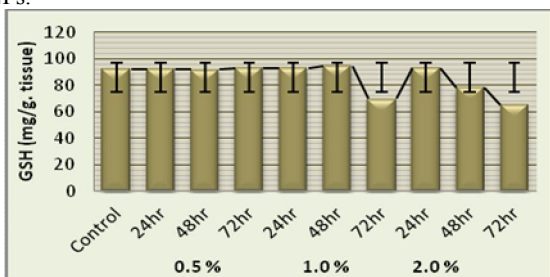


Figure (30): The mean  $\pm$  SD and significant differences ( $P < 0.05$ ) of GSH level in the skin of rabbits treated with TiO<sub>2</sub>-NPs.

The nonspecific esterase patterns of rabbit's skin treated with 0.5 % TiO<sub>2</sub>-NPs (group II) at the experimental exposure times of 24, 48 and 72hrs (lanes 2, 5 and 8) did not appear to be affected by treatment. No differences were distinguished in the banding distribution, the relative mobility values or even in the band intensities (Figs. 31, 32).

In rabbit's skin of group III (1.0 % TiO<sub>2</sub>-NPs), also no differences in the esterase banding patterns were noted at the 24hrs (lane 3) and 48hrs (lane 6) exposure times. Both treatments exhibited the six original bands (A1, A2, A3, B1, B2 and B3) seen in the control (Figs. 31, 32).

At 72hrs time period (lane 9), some changes were observed. Only five bands (A1, A2, A3, B1 and B2) were found, while the B3 band was missed. The five bands are similar to those found in the control. The only exception is B1 band was broad and exhibited a high staining intensity (Figs. 31, 32).

In the group IV (2.0 % TiO<sub>2</sub>-NPs) treated rabbits, no changes in the electrophoretic pattern of esterases could be observed at 24hrs of exposure (lane 4). All the six esterase bands (A1, A2, A3, B1, B2 and B3) of the control were expressed (Figs. 31, 32).

After 48 hrs of exposure (lane 7), three esterase bands were detected, the first two bands (A1 and A2) with relative mobilities of 0.49 and 0.58 respectively, were corresponding to that of the control. The third band (B1Ti) was marked at 0.79 Rm which did not line up with major esterase bands of the control (Figs. 31, 32). Moreover the A3, B1, B2 and B3 bands were absent as compared to the control.

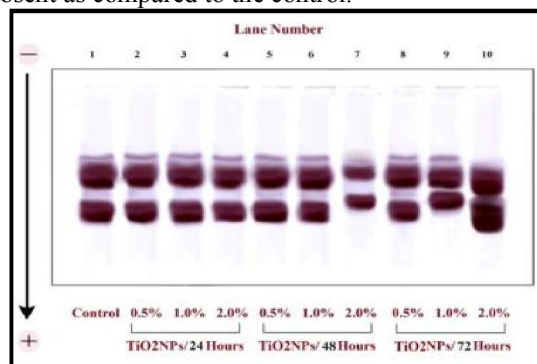


Figure (31): Polyacrylamide gel electrophoresis for esterases of the skin of rabbits using  $\alpha$ -naphthyl acetate substrate.

At 72hrs exposure time (lane 10), only four bands were obviously noted. The first three esterase bands (A2, A3 and B2) had electrophoretic mobilities more or less similar to the major bands of the control. The fourth esterase band (B4Ti) with 0.94 Rm is newly arises and did not match with esterase bands of the control. In addition, the A1, B1 and B3 bands were absent as compared to the control (Figs. 31, 32).

Generally, among the 8 bands, A2 was the most common band; it was expressed in all treatments, while B4 was specified only for the 2.0 % / 48 hr treatment and the B5 band was specified for 2.0 % / 72 hrs treatment.

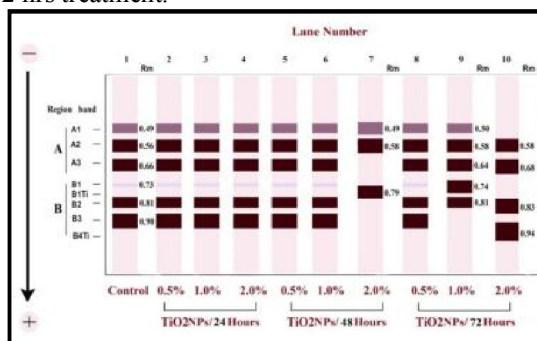


Figure (32): Illustration for the banding pattern of esterases detected in the above figure. A and B are the regions of esterase activity. Band size, intensity and relative mobility are shown.

### General Proteins Electrophoresis

SDS-PAGE for general proteins of the skin of rabbits treated with different concentrations of TiO<sub>2</sub>-NPs for 24, 48 and 72hrs Using Coomassie brilliant blue stain are displayed in the electrophoretic image (Fig. 34). An illustration for the banding pattern of proteins was constructed in an electropherogram to assess the changes of different treatments comparing to the control. The electropherogram is based on the calculated molecular weights (Fig. 35).

A total of 15 protein bands were recognized in the range from 94.5 to 20.0 KDa. The control pattern (lane 2) includes nine distinct bands with molecular weights of 94.5, 81.6, 65.8, 52.2, 46.8, 42.4, 32.2, 26.9 and 21.1 respectively. This is in comparison with the molecular marker (lane 1) values (Figs. 34 and 35).

On treatment with TiO<sub>2</sub>-NPs, Similar banding patterns were observed with 0.5% (group II) for all time periods (lanes 3, 6 and 9); with 1.0 % (group III) for 24hrs and 48hrs (lanes 4 and 7) and with 2.0 % (group IV) for 24hrs (lane 5). All the mentioned treatments exhibited all the nine protein bands of the control (lane 2) with a slight change in the molecular weight and intensity (Figs. 34 and 35).

In case of 1.0% TiO<sub>2</sub>-NPs / 72hrs, only seven bands could be identified (lane 10). Their molecular weights are ranged from 93.4 to 29.4 KDa. The three bands (44.8, 37.2 and 29.4 KDa) have no corresponding ones in the control, therefore they are considered abnormal bands. The remaining four bands are nearly similar to those of the control with a slight shift in mobility and intensity. In addition, five protein bands (46.8, 42.4, 32.2, 26.9 and 21.1 KDa) of the control were not expressed during the course of this treatment (Figs. 34 and 35).

Treatment with 2.0% TiO<sub>2</sub>-NPs (group IV) has a special interest, especially after 48hrs (lane 8) and 72hrs (lane 11) time periods. In both cases, the majority of bands were highly affected. In lane No.8, only six bands were detected, the fourth band (34.9 KDa) did not match the control, while the other five bands were more or less similar to those of the control although staining intensities were slightly different. In lane No.11, only four bands could be recognized. This represents the lowest number of bands among the other treatments. Two of the four bands (64.3 and 20 KDa) could have corresponding ones in the control, while the other two bands (48.3 and 40.6 KDa) did not line up with the control bands (Figs. 34 and 35).

### 4- Discussion

Nanotechnology seems to have a productive prospect for the future due to the realization that, the Nanoparticles (NPs) possess properties that differ significantly from those observed in bulk materials. However, as the outcome of unique properties of NPs, and because of increasing potential for exposure to

them, the potential biological hazard side effects should also be considered (Naseem *et al.*, 2014).

Although much progress has been made in explaining NPs toxicity, a satisfactory integration of the various experimental observations as well as a general description of the mechanism underlying NPs toxicity is extremely challenging, due to the wide variety of available data, complex interactions involved, broad range of engineered NPs (Sabella *et al.*, 2014).

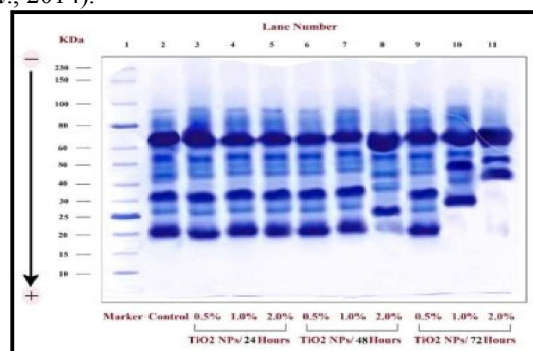


Figure (34): SDS-PAGE for general proteins of the skin of rabbits stained with Coomassie blue.

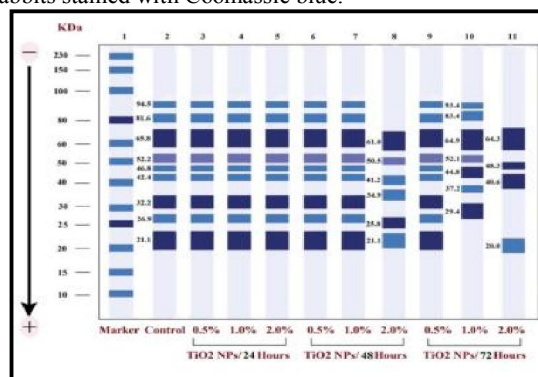


Figure (35): Illustration for the banding pattern of proteins detected in the above figure exhibiting band intensity, size and the appropriate molecular weights.

In the present work, the side effects of TiO<sub>2</sub>-NPs were studied at both the cellular and molecular levels. They particularly have attracted considerable attention in terms of Military Protection Wears (MPWs). The dermal impact of this NPs exposure was especially relevant due to its inclusion within MPWs that were directly in contact to skin.

The detail characterization of the TiO<sub>2</sub>-NPs was carried out. SEM image analysis was used for determining the shape and the average particle size. Hence, the examined NPs was spherical in shape and the average particle size was found to be 25 nm. On the other hand, the elemental composition as well as the purity of TiO<sub>2</sub>-NPs was examined by using the EDX and XRF analysis. The purity of TiO<sub>2</sub>-NPs was found to be 99.7 % and trace elements was detected as a little weight percents of impurities.

The present work did not illustrate any impact of TiO<sub>2</sub>-NPs at 0.5 % concentration after all the three exposure times (24, 48 and 72hrs), 1.0 % at 24 and 48hrs, as well as, 2.0 % concentration after 24hrs. The macroscopic examinations demonstrated that, topical application of TiO<sub>2</sub>-NPs of these concentrations did not affect the normal skin appearance where no lesions, scars, erythema or edema are recorded. In addition, light and electron microscope examinations showed normal histological structure with nearly no remarkable ultrastructure changes in the skin texture of the treated rabbits.

At the molecular level, the present work did not reveal any influence of these concentrations of TiO<sub>2</sub>-NPs on the glutathione enzymes. The activities of GST, GR, and the concentration of GSH did not show any significant differences from the control. In addition, the general protein banding patterns after the application of SDS-PAGE did not show difference in the banding profile of these concentrations of TiO<sub>2</sub>-NPs. Moreover, the nonspecific ESTs activity was investigated through the application of N-PAGE. Our results indicated that, ESTs pattern after the application of these concentrations did not show any differences as compared to control.

Our results indicated that, there was no evidence that TiO<sub>2</sub>-NPs of 0.5 % concentration after all the three exposure times (24, 48 and 72hrs), 1.0% at 24, 48hrs, and 2.0 % concentration after 24 hrs could penetrate into the deeper stratum corneum layer, epidermis or dermis. Thus the barrier function of the skin was successful in limiting the passage of particles. Consequently, our results suggest that the intact stratum corneum was an effective barrier to TiO<sub>2</sub>-NPs at these concentrations and the penetration of particles within the skin was negligible.

These results are in consistent with large set of *in vitro* and *in vivo* studies. The findings of the great majority of these studies illustrates that TiO<sub>2</sub>-NPs particles could not penetrate through the outermost layer of the intact stratum corneum with no distribution to the underlying living cell layers. The stratum corneum is therefore deemed to be an effective barrier against TiO<sub>2</sub>-NPs penetration in the skin. Therefore, the penetration of TiO<sub>2</sub>-NPs past the stratum corneum into viable skin layers is minimal (Pflucker *et al.*, 1999; Schulz *et al.*, 2002; Gamer *et al.*, 2006; Mavon *et al.*, 2007; Nohynek *et al.*, 2010; Christensen *et al.*, 2011).

On the contrary, the present work demonstrated well defined erythema and edemas during the macroscopic examination of the skin of rabbits after 72hrs exposure to 1.0 % concentration as well as, 48 and 72hrs exposure to 2.0 % concentration of TiO<sub>2</sub>-NPs. In addition, the rabbits appeared nervous with obvious jumpy movement and have a tendency to

excessive drinking. This might attributed to the inflammatory effect of TiO<sub>2</sub>-NPs on the skin. The excessive movements with the subsequent mechanical and flexing action on the skin might strength the irritative effect and provoke the dermal penetration of these NPs (Tinkle *et al.*, 2003; Lekki *et al.*, 2007; Rouse *et al.*, 2007; Zhang *et al.*, 2008; Larese *et al.*, 2009).

By the light and electron microscopes, our observations revealed several morphological changes after the application of these concentrations of TiO<sub>2</sub> NPs. The stratum corneum layer of the skin generally showed hyperkeratosis with decreasing in the thickness of the viable epidermis, this might attributed to the inhibition of the proliferation cycle. Where, the cell adhesion and proliferation was prevented as a result of exposure to TiO<sub>2</sub>-NPs (Jin *et al.*, 2008). In addition, Separations from the next granular layer were evident by the presence of many vacuolated areas.

At 72hrs exposure to 1.0 % TiO<sub>2</sub>-NPs, the stratum spinosum layer cells appeared shrunken with irregular or fragmented nuclei. Intercellular edema was evident by intercellular vacuolization, which explain the loss of the desmosomal connections and the increase in the intercellular separations. These cells also showed rupture of the nuclear and cellular membranes. These degenerative changes are signs of necrosis, where the affected cells seems unable to maintain the normal homeostasis and even incapable to perform the natural repair mechanism. TiO<sub>2</sub>-NPs exposure effects may occurs when the skin barrier functions were impaired and as a consequence, TiO<sub>2</sub> may come into direct contact with underlying skin cells. Moreover, the NPs were able to be internalized in the cytoplasm (Kiss, 2009).

At the 48hrs exposure to 2.0 % TiO<sub>2</sub>-NPs, the ultrastructure changes in the basal layer cells in addition to the degenerative changes in the granular and spinosum layers, indicated the penetration of these NPs to the deeper basal layer. The basal cells showed marked signs of necrosis evident by nuclear degeneration, as well as nuclear and cellular membranes rupture, and the cytoplasm appeared filled by many ruptured and swollen mitochondria. The basal lamina still well defined, with normal appearance of hemidesmosomes, and the dermis appeared with no changes.

On the other hand, the current work showed that increasing exposure time to the 72hrs lead to further penetration. The basal layer showed desmosomal dissolution and damaged hemidesmosomes, where intermediate filaments were not connected to the basal lamina. The basal lamina appeared discontinuous, broken, and lost its regular appearance. In addition the dermis appeared disorganized with closely packaged

thick collagen fibers. Numerous vacuolated areas and many fibroblasts that contained swollen and degenerated mitochondria were observed.

Our results indicated that, TiO<sub>2</sub>-NPs dermal penetration occurred as time and dose dependent, and the penetration was not limited to the stratum corneum, stratum granulosum and stratum spinosum. The TiO<sub>2</sub>-NPs may reach to the deeper basal layer and to the dermis. TiO<sub>2</sub>-NPs used in topical skincare products have been shown to be able to penetrate the stratum corneum barrier of the rabbit skin (Lansdown and Taylor, 1997).

Elsewhere, Tan *et al.* (1996) evaluated the epidermal penetration of TiO<sub>2</sub>-NPs into the epidermis using tape stripping. They found that levels of TiO<sub>2</sub>-NPs in the epidermis and dermis of subjects who applied TiO<sub>2</sub>-NPs to their skin were higher than the levels of TiO<sub>2</sub>-NPs found in controls. It is also worth noting that the morphology of the stratum corneum differs among different groups, which also influence the results. In addition, Bennat and Muller-Goymann (2000) observed that TiO<sub>2</sub>-NPs apparently penetrated deeper into human skin when applied as an oil-in-water emulsion, and that penetration was greater when applied to hairy skin, which suggest that TiO<sub>2</sub>-NPs penetrate surface through hair follicles or pores. The results of Wu *et al.* (2009) can at present be only accepted as preliminary, and speculative in terms of the hazard in humans, particularly. Since their findings in porcine skin *in vitro* and *in vivo* clearly indicate that TiO<sub>2</sub>-NPs (4nm and 60nm) penetrated into the stratum corneum, stratum granulosum, prickle cell layer and basal cell layer, but not into the dermis.

In the present work, the molecular examination may give explanation to the TiO<sub>2</sub>-NPs penetration mechanism. It has been shown that NPs may directly interact with lipid bilayer membranes, affecting thereby their stability. Moreover, formation of ion-selective pores in lipid bilayer as a consequence of NP interaction with membranes proteins has recently been reported (Planque *et al.*, 2011). Furthermore, the charge of NPs as well as their size and shape is likely to play a crucial role for interaction of NPs with lipid bilayer (Negoda *et al.*, 2013).

In the present work, the general protein banding patterns after the application of 1.0 % TiO<sub>2</sub>-NPs for 72hrs as well as, 2.0% concentration at 48 and 72hrs, displayed variation in the protein content of the skin extracts as revealed by SDS-PAGE. In both cases, the majority of the control bands were completely disappeared.

The primary mechanism of TiO<sub>2</sub>-NPs induced toxicity is due to oxidative stress, resulting in damage to cellular membranes and biological macromolecules including proteins and enzymes, as reported

earlier (Dalton *et al.*, 2002; Donaldson and Stone, 2003; Nel *et al.*, 2006; Shukla *et al.*, 2011).

According to these factors and according to our results, the penetration mechanism could be explained. The interaction of NPs with the cellular proteins may assist the passive transport of these NPs through the lipid bilayers and within the intercellular spaces, through disrupting the normal barrier property. Then the probability of entry of particles might be substantially increased (Donaldson and Stone, 2003; Shukla *et al.*, 2011).

In another approach, many studies revealed that; intracellular response to TiO<sub>2</sub>-NPs induced oxidative stress and caused generation of ROS with a significant reduction in the GSH levels in a dose and time dependent manner. ROS mediated oxidative stress as well as GSH depletion were found to be involved in the arresting of the cell cycle in G2/M phase and leading to apoptosis (Jin *et al.*, 2008; Saquib *et al.*, 2011; Shi *et al.*, 2013). In addition, the inhibition activities on the cells proliferation cycle (Suker *et al.*, 2013). From this point of view, the glutathione enzymatic activities were examined through our work as a good indicator for ROS mediated oxidative stress. In addition, might also give a good explanation for the disturbance of the proliferation cycle that lead to hyperkeratosis as illustrated in the microscopic examinations.

In the present work, the activities of GST and GR were increased in the rabbits skin treated with TiO<sub>2</sub>-NPs at the doses of 1.0 % (72hrs) and 2.0 % (48, 72hrs). On the other hand, the concentration of GSH was decreased. However, many earlier studies revealed that TiO<sub>2</sub>-NPs induced changes in the levels of oxidative markers especially depletion in the GSH level in dose dependent manner. This is mainly due to intracellular ROS generation and free radicals formation (Gurr *et al.*, 2005; Long *et al.*, 2007; Hussain *et al.*, 2009; Nemmar *et al.*, 2011). In addition to detoxification role of these enzymes, GSH also has antioxidant properties. Thus, GSH as a general stress indicator is a more useful diagnostic tool (Shukla *et al.*, 2011). Consequently, our data displayed a time and dose dependent effect of the TiO<sub>2</sub>-NPs treatments towards the enzymatic content of GST, GR and GSH in the skin of rabbits. Moreover, the results also revealed a positive correlation between the enzymatic activities of GST and GR, as well as a negative correlation of both enzymes with the GSH concentration.

Also, the cytotoxic responses of the rabbit skin extracts to the different concentrations of TiO<sub>2</sub>-NPs were surveyed by N-PAGE for monitoring the activity of general ESTs, as a good molecular and biochemical marker (Nascimento *et al.*, 2008; Memarizadeh *et al.*, 2014). TiO<sub>2</sub>-NPs at the doses of 1.0 % (72hrs) and 2.0

% (48, 72hrs) showed markedly inhibitory effect on the skin ESTs enzymes.

## References

- Bennat, C., and Muller, C.C.(2000). "Skin penetration and stabilization of formulations containing microfine titanium dioxide as physical UV filter," *Int. J. Cosmet. Sci.*, 22: 271–283.
- Beutler, E., Duron, O., Kelly, B.M. (1963). Improved method for the determination of blood glutathione. *J. Lab. Clin. Med.*, 61: 882 - 8.
- Christensen, F. M., Johnston, H.J., Stone, V., Aitken, R.J., Hankin, S., Peters, S., Aschberger, K. (2011) Nano-TiO<sub>2</sub> - feasibility and challenges for human health risk assessment based on open literature. *Nanotoxicol.* 5(2): 110-124.
- Dalton, P., Doolittle, N., Paul, A.S. (2002). Gender specific induction of enhanced sensitivity to odors. *Nature. Neurosci. J.*, 5: 199 – 200.
- Dastjerdi, R. and Montazer, M. (2010). "A review on the application of inorganic nano structured materials in the modification of textiles: Focus on anti-microbial properties," *Coll and Surf. B: Biointerfaces.*, 79: 5–18.
- Davis, B. J. (1964), Disc Electrophoresis – II Method and Application to Human Serum Proteins. *Ann New York Acad Sci.*, 121: 404–427.
- Dechsakulthorn, F., Hayes, A., Bakand, S., Joeng, L., and Winder, C. (2007). "In vitro cytotoxicity assessment of selected nanoparticles using human skin fibroblasts," *AATEX*, 14, Special Issue: 397-400.
- Donaldson, Ken., and Stone, Vicki. (2003). Current hypotheses on the mechanisms of toxicity of ultrafine particles. *Ann. Ist. Super. Sanità.*, 39(3):405-410.
- Dussert, A.S., and Gooris, E. (1997). "Characterisation of the mineral content of a physical sunscreen emulsion and its distribution onto human stratum corneum," *Int. J. Cosmet. Sci.*, 19:119-129.
- Gamer, A.O., Leibold, E., and van R.B.(2006) "The *in vitro* absorption of microfine zinc oxide and titanium dioxide through porcine skin," *Toxicol. In Vitro. J.*, 20: 301–307.
- Goldberg, D.M., and Spooner, R.J. (1983). *Methods of. Enzymatic Analysis.* (Bergmeyer, H.V. Ed.). 3rd ed. vol 3: pp 258-265.
- Gurr, J.R., Wang, A.S., Chen, C.H., Jan, K.Y. (2005) Ultrafine titanium dioxide particles in the absence of photoactivation can induce oxidative damage to human bronchial epithelial cells. *Toxicol. J.*, 213(1–2):66–73.
- Habig, W.H., Pabst, M.J., Jacoby, W.B. (1974). Glutathione S-transferase, The first enzymatic step in mercapturic acid formation. *J Biol Chem.*, 249: 7130–7139.
- Hussain, M., Rao, M., Humphries, A.E., Hong, J.A., Liu, F., Yang, M., Caragacianu, D., Schrumpp, D. S. (2009). Tobacco smoke induces polycomb-mediated repression of Dickkopf-1 in lung cancer cells. *Cancer Res.*, 69:3570–3578.
- Jeevani, T. (2011). "Nanotextiles- A Broader Perspective," *Nanomedic. Nanotechnol. J.*, Vol 2: 7-1000124.
- Jin, C., Zhu, B., Wang, X., Lu, Q.(2008) "Cytotoxicity of titanium dioxide nano-particles in mouse fibroblast cells," *Chem. Res. Toxicol. J.*, 21:1871-1877.
- Kiss, B. (2009). "Investigation of micronized titanium dioxide penetration in human skin xenografts and its effect on cellular functions," *Ph. D.Thesis. Debrecen. Univ.*
- Lademann, J., Weigmann, H.J., Rickmeyer, C., Barthelmes, H., Schaefer, H., Mueller, G., Sterry, W. (1999). Penetration of titanium dioxide microparticles in a sunscreen formulation into the horny layer and the follicular orifice. *Skin Pharmacol Physiol.*, 12:247–256.
- Laemmli, U.K. (1970). Cleavage of structural proteins during the assembly of the head of bacteriophage P4. *Nature.*, Vol. 227. 680-686.
- Lansdown, A.B.G., and Taylor, A. (1997). Zinc and titanium oxides: promising UV-absorbers but what influence do they have on intact skin? *Int. J. Cosmet. Sci.*, 19, 167–172.
- Mavon, A., Miquel, C., Lejeune, O., Payre, B., Moretto, P. (2007). "In vitro percutaneous absorption and in vivo stratum corneum distribution of an organic and a mineral sunscreen," *Skin. Pharmacol. Physiol. J.*, 20: 10-20.
- Naseem, S., Gatoo, M.A., Dar, A.M., Qasim, K. (2014). IN VIVO TOXICITY OF NANOPARTICLES: MODALITIES AND TREATMENT. *Eur. Chem. Bull.*, 3(10): 992-1000.
- Negoda, A., Kwang-Jin, K., Edward, D. C., Robert, M. W. (2013). Polystyrene nanoparticle exposure induces ion-selective pores in lipid bilayers. *Biochimica et Biophysica Acta.*, 1828: 2215–2222.
- Nel, A., Xia, T., Madler, L., Li, N. (2006). Toxic potential of materials at the nano-level. *Nano. Sci. J.*, 311:622–7.
- Nemmar, A., Al-Salam, S., Zia, S., Marzouqi, F., Al-Dhaheer, A., Subramanian, D., Kazzam, E. E. (2011). Contrasting actions of diesel exhaust particles on the pulmonary and cardiovascular systems and the effects of thymoquinone. *British. J. Pharmacol.*, 164(7): 1871–1882.
- Nohynek, G. J., Antignac, E., Thomas, Re., Toutain, H. (2010). Safety assessment of personal care products/cosmetics and their ingredients. *Toxicol. Appl. Pharmacol.*, 1;243(2):239-59.
- Pflucker, F., Hohenberg, H., Holzle, E., Will, T., Pfeiffer, S., Wepf, R., Diembeck, W., Wenck, H., Gers-Barlag, H., (1999). "The outermost stratum corneum layer is an effective barrier against dermal uptake of topically applied micronized titanium dioxide," *Int. J. Cosmet. Sci.*, 21: 399–411.
- Planque, M.R.R., Aghdaei S., Roose, T., Morgan, H. (2011). Electrophysiological characterization of membrane disruption by nanoparticles. *ACS Nano.*, 5 (5), pp 3599–3606.
- Sabella, S., Randy, P. Carney., Virgilio, B., Maria, A. d. M., Noura, Al- J., Giuseppe, V., Sam, M. J., Osman, M. B., Roberto, C., Francesco, S., Pier, P. P. (2014). A general mechanism for intracellular toxicity of metal-containing nanoparticles. *Nanoscale.*, 6: 7052–7061.
- Sadrieh, N., Wokovich, A.M., Gopee, N.V., Zheng, J., Haines, D., Parmite, D., Siitonen, P.H., Cozart, C.R., Patri, A.K., McNeil, S.E., Howard, P.C., Doub, W.H., Buhse, L.F. (2010). "Lack of Significant Dermal Penetration of Titanium Dioxide from Sunscreen Formulations Containing Nano- and Submicron-Size TiO<sub>2</sub> Particles," *Toxicol. Sci. J.*, 115: 1, 156–166.
- Saqib, Q., Al-Khedhairi, A.A., Siddiqui, M.A., Abou-Tarboush, F. M., Azam, A., Musarrat, Javed. (2011). "Titanium dioxide nanoparticles induced cytotoxicity, oxidative stress and DNA damage in human amnion epithelial (WISH) cells," *Toxicol In Vitro.*, 26:351–361.
- Satam, D.S., (2007). "Global competitiveness of USA military textiles industry," *Glob. Text and Apparel Mark.*, 21:173-82.
- Schulz, J., Hohenberg, H., Pflucker, F., Gärtner, E., Will, T., Pfeiffer, S., Wepf, R., Wendel, V., Gers-Barlag, H., Wittern, K. P. (2002). Distribution of sunscreens on skin. *Adv. Drug. Deliv. Rev.*, 54(1): 157-163.
- Senic, Z., Bauk, S., Todorović, M., Pajić, N., Samolov, A., and Rajić, D. (2011). "Application of TiO<sub>2</sub> nanoparticles for obtaining self-decontaminating smart textiles," *Scientific Technical Review.*, 61: 3-4, 63-72.
- Senzui, M., Tamura, T., Miura, K., Ikarashi, Y., Watanabe, Y., and Fujii, M. (2009). "Study on penetration of titanium dioxide (TiO<sub>2</sub>) nanoparticles into intact and damaged skin in vitro," *J. Toxicol. Sci.*, 35: 1, 107-113.
- Shi, H., Magaye, R., Castranova, V., and Zhao, J. (2013). "Titanium dioxide nanoparticles: a review of current toxicological data," *Particle and Fibre Toxicol.*, 10:15.
- Shukla, G.C., Haque, F., Tor, Y., Wilhelmsson, L. M., Toulme, J. J., Isambert, H., Guo, P., Rossi, J. J., Tenenbaum, S. A., Shapiro, B. A. (2011). A boost for the emerging field of RNA nanotechnology. *ACS Nano* 5: 3405–3418.
- Suker, D.K., Reyam, M., Ibadran, A.(2013). "Cytotoxic effects of titanium dioxide nano-particles on rat embryo fibroblast (REF-3) cell-line *in vitro*," *Euro. J. Exp Biol.*, 3(1):354-363.
- Tan, M., Commens, G.A., Burnett, L., Snitch, P.J. (1996). "A pilot study on the percutaneous absorption of microfine titanium dioxide from sunscreens," *Aust. J. Dermatol.*, 57: 185-187.
- Wong, Y. W. H. (2006). "Characterization of Nano-treated materials using advanced instrumental techniques," *Master of Philosophy Thesis, Hong Kong Polytechnic University.*
- Wu, J., Liu, W., Xue, C., Zhou, S., Lan, F., Bi, L., Xu, H., Yang, Z., and Zeng, F. D.(2009). "Toxicity and penetration of TiO<sub>2</sub> nanoparticles in hairless mice and porcine skin after subchronic dermal exposure," *Toxicol. Lett.*, 191: 1–8.